PRESSURE AND SHEAR RESPONSES IN BRAIN INJURY MODELS

D. R. S. Bradshaw[*,†]
C. L. Morfey[*]
[*]ISVR, University of Southampton, UK
[†]First Technology, USA
274

ABSTRACT

Finite element (FE) models of the brain are regularly used to investigate brain injury mechanisms. Validation of these models against cadaver impacts is usually restricted to intracranial pressure data. However, the low shear modulus of neural tissue means that injurious strains result from shear deformations. We show that brain injury models that are validated for pressure alone can give a wide range of shear responses to the same impact.

Holbourn's arguments on the harmlessness of pressure are extended by introducing separate wave equations for pressure and shear, derived from the Helmholtz vector decomposition. Two idealised models of traumatic brain injury are used to show that there is no one-to-one relation between pressure and shear in head impacts lasting a few milliseconds. The first is an analytical model of wave propagation in the brain under the action of local skull bending. The second is a strain-validated FE representation of the coronal plane of the human head under rotational acceleration.

As there is no one-to-one relation between dilatation and distortion in typical head impacts, it is not acceptable to validate FE models for pressure and then use them to predict injury.

INTRODUCTION

In the early 1940's, Holbourn argued that the controlling parameters for traumatic brain injury (TBI) are skull bending, skull fracture and rotation of the head [7,8]. His arguments were strongly founded on Newton's laws of motion and were derived mainly from observations regarding the material properties of cerebral tissue. Although many researchers have cited the research, his arguments and conclusions regarding the harmlessness of pressure seem largely to have been disregarded.

In the present article, Holbourn's arguments are developed further with the introduction of wave equations for pressure and shear (Equations 10 and 11), which themselves are derived from the Helmholtz vector decomposition of the displacement field (Equation 9). We will show that, for peculiar materials like brain tissue, there is no one-to-one relation between pressure and shear in impacts lasting a few milliseconds. This has serious implications for testing of FE models.

The arguments developed in this article are most relevant to those brain injuries that are caused by excessive stretching of neural tissue. They are therefore principally directed towards diffuse axonal injuries (DAI). Injuries caused by skull fracture or penetration are not covered, neither are injuries caused by excessive motion of the cerebrum within the cranial vault, such as acute subdural haematoma (ASDH).

DILATATION AND DISTORTION

Holbourn's arguments derived from the observation that the brain is far more resistant to compression than to shear. The compression, or dilatation (Δ), of a small tissue element is given by

$$\Delta = \delta V / V_0 , \qquad (1.)$$

where δV is the volume change and V_0 is the initial volume (Figure 1a).

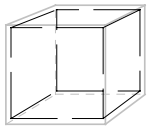

a) Dilatation (compression)

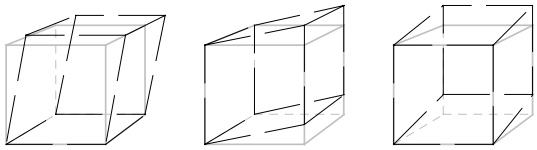

b) Distortion (shear)

Figure 1.

Schematic diagram of dilatational and distortional strains in a small sample of brain tissue.

The dilatation is related to the pressure (p) and the bulk modulus of a material (K) by the expression

$$p = -K\Delta . \qquad (2.)$$

The bulk modulus of cored samples of the human brain is 2.07 GPa, which is not significantly different to that

of water [13]. Thus, the typical peak positive pressures encountered in TBI (200 kPa to 500 kPa) generate very small dilatational strains (1×10^{-4} to 2×10^{-4}).

In contrast to the unique description of dilatation, there are several different descriptions of shear strain, or distortion (ε'). The description used here is the Lagrangian shear strain, which is approximately equal to half the angle γ in Figure 2.

$$\varepsilon' = \gamma / 2 \,. \tag{3.}$$

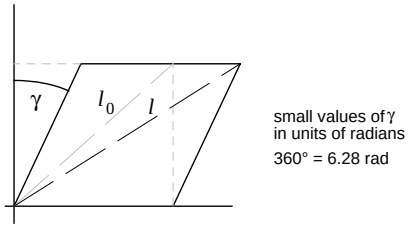

Figure 2.

Schematic diagram of distortional strain in 2D.

The distortional strain is related to the shear stress (σ') and the shear modulus (μ) by the expression

$$2\varepsilon' = \gamma = \sigma' / \mu \,. \tag{4.}$$

The shear modulus of cored samples of human brain is time dependent, but lies in the range 1 kPa to 10 kPa, approximately a million times smaller than the bulk modulus [5]. Typical distortional strains measured in physical models of TBI are of the order (1×10^{-2} to 2×10^{-1}) [4,10,12,14]. Thus, in brain injury, dilatational strains are approximately a thousand times smaller than distortional strains.

Tissue level models have successfully shown that axonal injury is initiated by the physical process of extension or stretching [1,2]. The maximum principal strain (ε_{I}) is a measure of the maximum stretch that a neuron experiences, and therefore is a good injury predictor. In the 2D example shown in Figure 2, the maximum principal Lagrange strain is given by

$$\varepsilon_{\mathrm{I}} = 0.5\left(\left(l / l_0\right)^2 - 1\right). \tag{5.}$$

As the volumetric strains in TBI are extremely small by comparison with distortional strains, we can deduce certain relations between distortional strains and the maximum principal strain. In 2D (Figure 2), the relation is very simple. It is given by

$$\varepsilon' \simeq \varepsilon_{\mathrm{I}} \,. \tag{6.}$$

In 3D (Figure 1), the relation is more complex as there are now three distortional strains. The maximum shear strain ($\varepsilon'_{\max}$) is a measure of the greatest shear at a point. The relation between maximum distortional and maximum principal strain is given by

$$\tfrac{2}{3}\varepsilon'_{\max} < \varepsilon_{\mathrm{I}} < \tfrac{4}{3}\varepsilon'_{\max} \,. \tag{7.}$$

In summary, there are minor differences (less than a factor of 2) between maximum shear strain and maximum principal strain in TBI problems. However, we can state categorically that the dilatation is far smaller than both of these, by a factor of approximately 1 000. The principal purpose of this article is to demonstrate that there is no relation between the maximum principal strain and the pressure during closed head injury, and therefore that pressure is not suitable as a model testing parameter.

WAVE EQUATIONS

The effects of a localised force applied abruptly to a point in a medium soon transmit to other parts of the medium. This simple fact forms the basis of study of impact problems from the perspective of wave propagation.

Two distinct wave types propagate through a material under dynamic loading: dilatational and distortional waves. The two wave types propagate at different speeds, c_{d} and c_{s}, respectively given by:

$$\text{(dilatation)} \quad c_{\mathrm{d}} = \left(\left(K + \tfrac{4}{3}\mu\right)/\rho\right)^{1/2}, \tag{8a.}$$

$$\text{(distortion)} \qquad c_{\mathrm{s}} = \left(\mu/\rho\right)^{1/2}. \tag{8b.}$$

where ρ is the mass density.

Associated with each point in a medium is a local displacement vector , $\boldsymbol{u}$, which may be split into two parts: $\nabla\phi$ for the dilatational wave component, and $\nabla \times \boldsymbol{\Psi}$ for the distortional component. Thus,

$$\boldsymbol{u} = \nabla\phi + \nabla \times \boldsymbol{\Psi} \,. \tag{9.}$$

The ϕ and $\boldsymbol{\Psi}$ functions are called the scalar and vector potentials of $\boldsymbol{u}$; they obey the separate wave equations

$$\nabla^2\phi = \frac{1}{c_{\mathrm{d}}^2}\frac{\partial^2\phi}{\partial t^2}, \tag{10.}$$

$$\nabla^2 \boldsymbol{\Psi} = \frac{1}{c_s^2} \frac{\partial^2 \boldsymbol{\Psi}}{\partial t^2} . \qquad (11.)$$

Pressure and shear waves in the brain

A typical value of c_d for either grey or white matter is 1 410 m·s^{-1}. This is so large that a pressure pulse can travel across the cranial diameter about 10 times per millisecond. Therefore, in blunt head impacts, where the duration is generally 2 ms or more, the pressure response within the head arrives at hydrostatic equilibrium almost instantaneously. In this case, the pressure is dependent only on the density of the material, and not on its shear or bulk modulus. The pressure distribution in the brain is of the form

$$p \simeq -\rho h \ddot{u} . \qquad (12.)$$

The consequences are illustrated for a translational frontal impact to the head in Figure 3. The instantaneous pressure within the brain follows a linear variation with position, falling from 151 kPa at the front (coup) to -76 kPa at the rear (contrecoup). The head acceleration and cranial dimensions are chosen to match the moment of peak force in the cadaver impact experiment of Nahum (1977), and are shown on the figure [13].

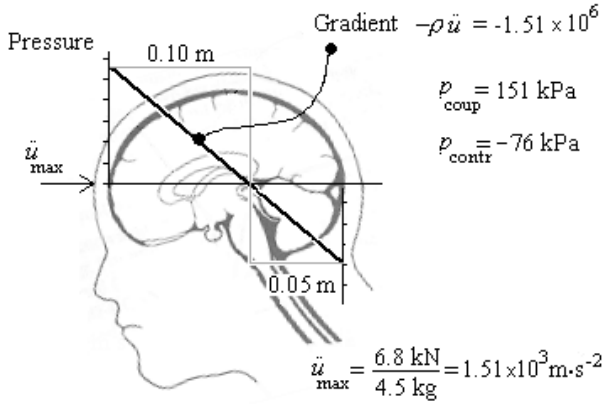

Figure 3.

Schematic diagram of linear pressure variation hypothesis. The figure shows the predicted pressure distribution at the moment of peak loading from a cadaver impact experiment conducted by Nahum (1977).

Further evidence to support these observations may be found in Thomas et al. (1967) [16].

Typical values of c_s are three orders of magnitude lower than c_d: c_s = 1.5 m·s^{-1} to 2 m·s^{-1}. The ratio of the two wavespeeds C (c_s / c_d) is of order 10^{-3}. The transit time for a shear wave pulse crossing the cranium is of order 100 ms, a long time on the blunt head impact timescale. As principal strains are dominated by shear strain, wave effects can therefore be expected to play a dominant role in TBI.

Hypothesis that pressure and shear are controlled by unrelated material parameters

Guided by these observations, we arrive at a hypothesis concerning pressure and shear in TBI and their dependence on material properties. We postulate that, for any given motion of the skull that is consistent with closed head impact (blunt impacts, no depressed fracture or penetration), separate tissue parameters determine the two responses of transient intracranial pressure (ICP) and maximum principal strain (ε_I). Specifically:

- ICP time-history at any point in the brain following impact is independent of tissue elastic properties (K, μ) for typical translational impacts (duration > 2 ms), but is dependent on the density.
- The principal strain time-history at any point in the brain following impact is dependent almost entirely on distortional wave speed c_s.

In the following sections of this article, the hypothesis will be tested against accurate predictions from two specific brain injury models, in which the geometry has been simplified to permit reliable calculations of dilatation and distortion. The first model is analytical and considers the situation where the driving mechanism is local skull deformation. The second is numerical (FE) with experimental validation, and considers rigid skull rotation as the driving mechanism.

Implications of the hypothesis

If the hypothesis above can be validated for the typical range of blunt head impacts, there are significant implications for FE models of TBI. Required inputs for FE models are the shear and compressional wavespeed of neural tissue. Researchers often adjust these parameters to achieve agreement between cadaver-impact pressure data and the FE simulation.

If pressure is the only test variable, validation for principal strain is impossible: the principal strain depends critically on tissue values that have no bearing on the pressure. Recall here that is it principal strains that cause injury, not dilatational.

SKULL DEFORMATION MODEL

The hypothesis will be tested first against an analytical model designed to capture the physics of wave transmission within the cerebrum and subarachnoid layer, under the action of local skull deformation.

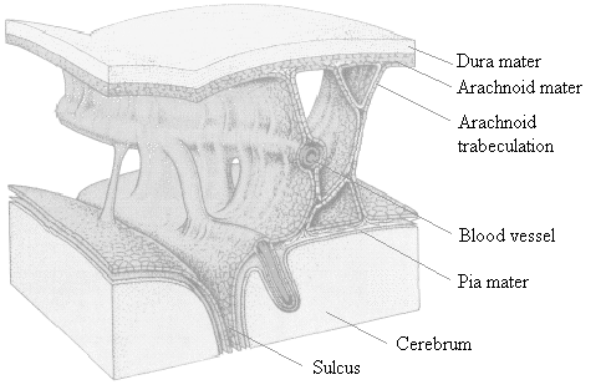

Figure 4.

Diagram of the subarachnoid space. Note the arachnoid trabeculations and cerebral blood vessel. Adapted from Gray (1995) [6].

The analytical model includes a representation of the subarachnoid space, containing the cerebrospinal fluid (CSF) and the arachnoid trabeculations, as well as the cerebrum (Figure 4).

A plane boundary, representing the inner surface of the skull, vibrates in the normal (x_2) and tangential (x_1) directions (Figure 5).

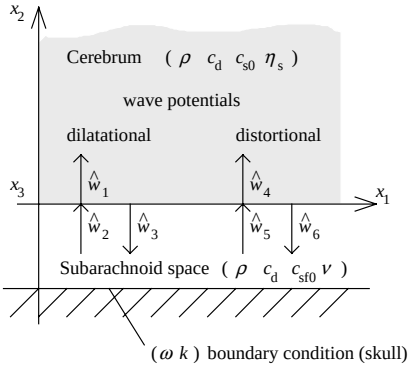

Figure 5.

The boundary represents the skull, a fluid layer represents the subarachnoid space (containing CSF and trabeculae) and the semi-infinite medium represents the cerebrum.

The relations between material parameters and dilatational and distortional wavespeeds in the cerebrum are summarised by the following expressions:

$$c_{\mathrm{d}}^2 = \frac{\lambda + 2\mu}{\rho} = c_{\mathrm{d0}}^2\left(1 + \mathrm{j}\eta_{\mathrm{d}}\right). \tag{13.}$$

were the Lamé constant $\lambda = K - \frac{2}{3}\mu$, and η_{d} is the frequency dependent loss factor.

$$c_{\mathrm{s}}^2 = \frac{\mu}{\rho} = c_{\mathrm{s0}}^2\left(1 + \mathrm{j}\eta_{\mathrm{s}}\right). \tag{14.}$$

In the fluid layer we have:

$$c_{\mathrm{df}}^2 = \frac{\lambda_{\mathrm{f}} + 2\mu_{\mathrm{f}}}{\rho_{\mathrm{f}}} = c_{\mathrm{df0}}^2\left(1 + \mathrm{j}\eta_{\mathrm{df}}\right), \tag{15.}$$

$$c_{\mathrm{sf}}^2 = \frac{\mu_{\mathrm{f}}}{\rho_{\mathrm{f}}} = c_{\mathrm{sf0}}^2\left(1 + \mathrm{j}\eta_{\mathrm{sf}}\right). \tag{16.}$$

In Figure 5 we have introduced the assumptions that the densities and dilatational wave speeds in the two layers are the same. The constraints are added primarily to simplify the problem, and also because these parameters are not the focus of the study. Thus

$$\rho_{\mathrm{f}} = \rho, \text{ and } c_{\mathrm{df}} = c_{\mathrm{d}} \tag{17.}$$

so
$$\lambda_{\mathrm{f}} + 2\mu_{\mathrm{f}} = \lambda + 2\mu = \rho c_{\mathrm{d}}^2. \tag{18.}$$

The problem is further simplified by requiring that c_{d} be real (i.e. $\eta_{\mathrm{d}} = 0$). These assumptions reduce the number of independent material parameters to six: ρ, c_{d}, c_{s} and c_{sf} (both complex).

The shear material parameters for the subarachnoid space arise from a combination of the CSF, which is modelled as a Newtonian fluid with kinematic viscosity ν, and the trabeculae, which contribute a small elastic component, G_{f}. Thus

$$c_{\mathrm{sf}}^2 = \frac{\mu_{\mathrm{f}}}{\rho} = c_{\mathrm{sf0}}^2\left(1 + \mathrm{j}\eta_{\mathrm{sf}}\right), \tag{19.}$$

where
$$\mu_{\mathrm{f}} = G_{\mathrm{f}} + \mathrm{j}\omega\rho\nu. \tag{20.}$$

To summarise, the properties of both media are now completely specified in terms of ($\rho, \nu, c_{\mathrm{d}}, c_{\mathrm{s0}}, \eta_{\mathrm{s}}, c_{\mathrm{sf0}}$).

Solution to analytical model

The solution to the analytical model is given in concise form in Appendix A. The complete derivation of

displacements, velocities, strain and stress fields and dimensional analysis can be found in Bradshaw (2001).

The output dilatation and distortion are a function of the non-dimensional input groups $\{C, S, Ma_t, Re, \eta_s, \gamma\}$, where the group of interest here is C, the ratio of the wavespeeds in the cerebrum c_{s0}/c_d. Typical values are used for the other groups. A more thorough investigation of the model is presented elsewhere [3].

Results from analytical model

Focusing on the dilatation amplitude and not its phase, graphs are presented for the real quantities

$$\begin{aligned} Z_1 &= \left|\hat{Z}_1\right| \\ Z_2 &= \left|\hat{Z}_2\right| \end{aligned} . \qquad (21.)$$

where $\hat{Z}_1$ and $\hat{Z}_2$ are the complex transfer functions between the velocity input boundary condition ($\hat{v}_1$ and $\hat{v}_2$) and the dilatation in the cerebrum.

From Appendix A we note that the peak maximum distortion ($\tilde{e}_{\text{peak}}$) is a non-linear function of the complex response functions $\left\{\hat{D}_1, \hat{D}_2, \hat{E}_1, \hat{E}_2\right\}$. Consequently, graphs are presented for the real quantities

$$\begin{aligned} E_1 &= \frac{\tilde{e}_{\text{peak}}\left(\hat{v}_1\right) \cdot c_d}{\left|\hat{v}_1\right|} \\ E_2 &= \frac{\tilde{e}_{\text{peak}}\left(\hat{v}_2\right) \cdot c_d}{\left|\hat{v}_2\right|} \end{aligned} . \qquad (22.)$$

Figure 6 contains two graphs that show how the non-dimensional dilatation and distortion vary as a function of C, the real wavespeed ratio. Panel 'a' shows the responses for a tangential velocity boundary condition, while panel 'b' shows the responses for a normal velocity boundary condition. In each case, C is varied by one decade either side of the typical value ($C = 10^{-3}$). This is equivalent to varying μ by four decades whilst holding K constant.

The fact that there is a flat response for the dilatation while the distortion varies is clear evidence that there is no one-to-one relation between dilatation and distortion in this model.

Clearly, many further investigations could be pursued with the analytical model. For example, we can investigate the effect of the thickness of the subarachnoid space on the coupling between the skull and the brain, or the effect of the elasticity provided by the arachnoid trabeculations. In addition, the response at a range of trace Mach numbers might be sought. These investigations are all presented in Bradshaw (2001).

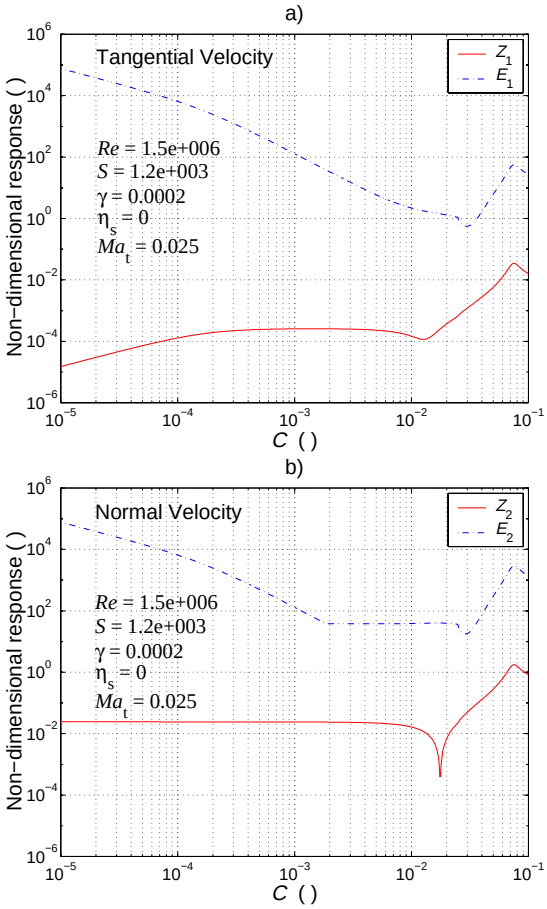

Figure 6.

Non-dimensional dilatation and maximum distortional response as a function of C, the ratio of real wave speeds, c_{s0}/c_d.

SKULL ROTATION MODEL

The second model was designed to capture the physics of brain deformation driven by rotation of the whole head in the coronal plane. A 2D FE model (Figure 7), with a slip boundary condition over most of the skull interior, contains a representation of the falx, the sulci and the cerebrum.

The model was developed in LS-DYNA [11], an explicit FE code capable of non-linear behaviour. 2D plane-strain element formulations were used.

The geometry was based on measurements taken from MRI scans. Justification for the circular approximation to the brain geometry in the mid-coronal plane, and the extent of the no-slip boundary condition, is shown in

Figure 8. Further details of the physical model geometry can be found elsewhere [4]. At least 10 elements per wavelength are required for a maximum 2 % error [3]. HyperMesh [9] was used to generate an FE mesh with a characteristic element size of 1 mm that, together with the material properties detailed below, results in a model that can accept input energy at frequencies up to 200 Hz (see Figure 7).

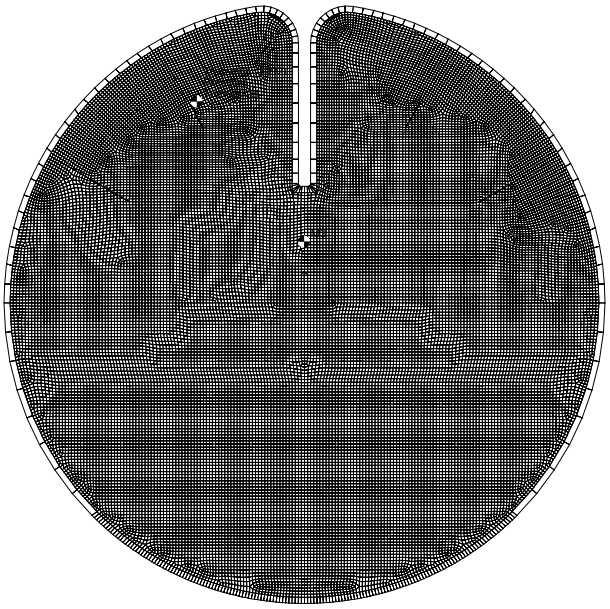

Figure 7.

Schematic diagram of FE model of coronal plane. The position of the Patrick marker in the corpus callosum is highlighted: M3=(0,19).

Material models

The material properties of the cerebrum were approximated by a three-parameter Boltzmann model. Volumetric strains are elastic, and deviatoric strains are viscoelastic with shear relaxation behaviour described by an impulse response function

$$G(t) = G_\infty + \left(G_0 - G_\infty\right)\mathrm{e}^{-\beta t}. \qquad (23.)$$

The available test data on the gel are limited to the frequency range 1 Hz to 20 Hz [10]. An acceptable fit between experimental data and an FE material model is found using G_0 = 3 846 Pa, G_∞ = 893 Pa and β = 187 s^{-1} [3].

The sulci were represented by 0.2 mm sheets of an elastic material (E = 20 MPa, υ = 0.3, $\rho = 1 \times 10^3$ kg·m^{-3}). An elastic material model was also used for the aluminium skull (E = 700 MPa, υ = 0.3, $\rho = 274 \times 10^3$ kg·m^{-3}). The properties used for the aluminium where chosen to improve the timestep of the solution. The difference has no effect on the results.

Boundary conditions

Representing the boundary condition between the brain and the skull has been a perennial problem in FE models. A satisfactory solution has been found here in the form of a 2D sliding only contact. This contact allows frictionless slip between the skull and the brain, without unrealistic separation of the two materials or gross element deformation.

The model was tested by comparing nodal displacements and strain output with data obtained from physical model experiments reported in Bradshaw et al. (2001). Comparisons can be found in Bradshaw (2001).

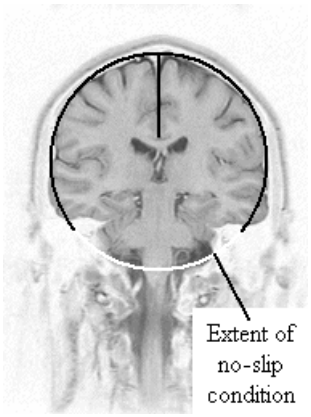

Figure 8.

MRI scan of mid-coronal plane through the brainstem. Note the circular approximation to the geometry in this plane and the extent of the no-slip boundary condition in the skull base.

FE model output

Rectangular Cartesian axes $OX_1X_2X_3$ were defined with their origin at the centre of rotation of the model. The axes rotated with the aluminium vessel, so that displacements were calculated with respect to the skull. The nodal position and strain at M3, highlighted with a Patrick marker in Figure 7, were extracted from the FE output database.

Analyses completed

The model was loaded with the rotational acceleration time-history shown in Figure 9. The impact is characterised by a peak angular acceleration of 7 800 rad·s^{-2}, which roughly corresponds to a serious brain injury threshold in man.

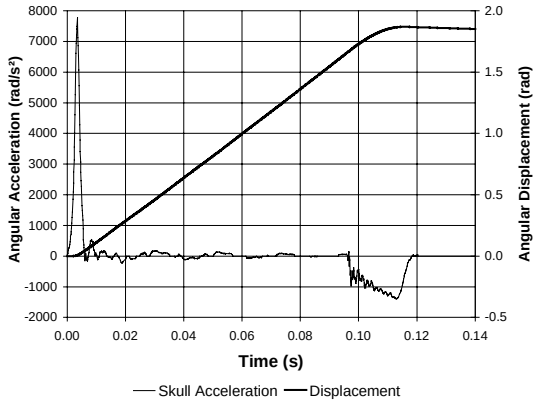

Figure 9.

Skull kinematics. Angular acceleration and angular displacement of the skull are shown for a typical experiment (filtered with SAE C1000).

Three analyses were completed using different values for the shear material properties of the brain. The short and long term shear moduli were varied by a factor of 10 either side of typical value for human tissue (see Table 1). All other parameters were unchanged.

Table 1.

Summary of cerebral material properties used

	C	K (MPa)	G_0 (Pa)	G_∞ (Pa)	β (s^{-1})
I	1.4×10^{-3}	210	385	89	187
II	4.3×10^{-3}	210	3 846	894	187
III	1.4×10^{-2}	210	38 460	8 936	187

Results from FE numerical analyses

Figure 10a shows the pressure time-history predicted at M3 in the corpus callosum, for analyses I, II and III. The peak pressures from the three analyses are indistinguishable from each other (25 kPa), despite the wide variation in the shear modulus of the brain. Generally, the pressures in the three simulations are lower than intracranial pressure measurements made during cadaver impacts, and nowhere exceed 30 kPa [15,17]. The principal reason is that the acceleration input in the simulation was purely rotational.

Figure 10b shows the predicted maximum principal strain response at M3 for analyses I, II and III. The peak strains during the first 50 ms of each analysis are 0.578, 0.228 and 0.059 for G_0 = 0.39 kPa, 3.9 kPa and 39 kPa respectively. To a good approximation, the peak strain response is inversely proportional to $\sqrt{G_0}$.

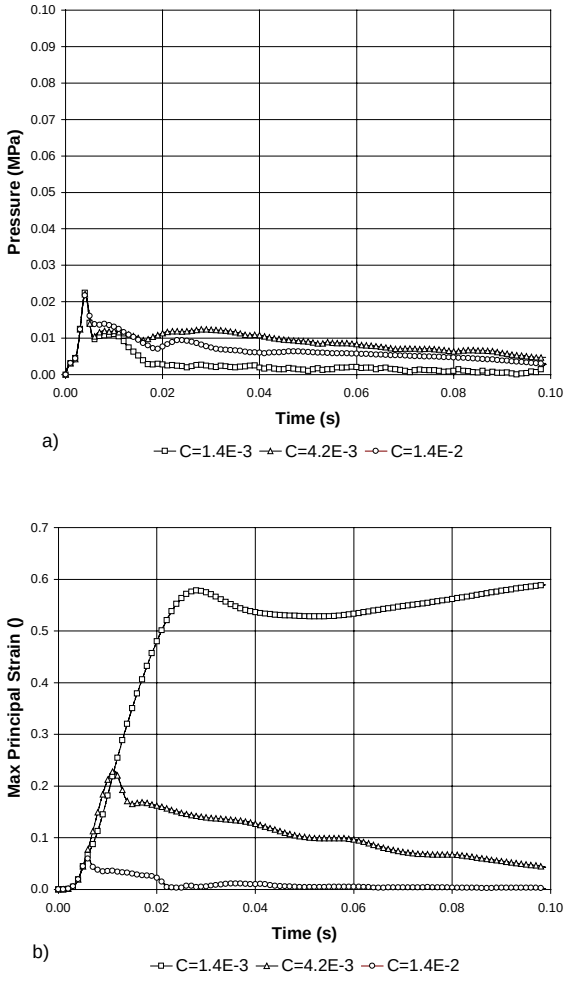

Figure 10.

Summary of results from analyses I, II and III: Pressure and maximum principal strain time histories for M3, in the corpus callosum.

Thus varying shear material properties by an order of magnitude, above and below baseline values that are appropriate for human cerebral tissue, produces little change in the pressure response in an FE model of TBI. At the same time, the peak maximum principal strain is very sensitive to changes in shear modulus.

DISCUSSION

We have noted that the bulk modulus of the cerebrum is approximately 10^6 times larger than the shear modulus. There are several direct consequences:

- The dilatational (pressure) wavespeed is ~10^3 times faster than distortional.

- Dilatational strains in the cerebrum are ~10^4 times smaller than distortional.
- The maximum principal strain is approximately equal to the maximum shear strain.

Tissue level models of DAI have successfully shown that injury is a function of strain [1,2]. Given the relative magnitudes of the dilatational and distortional components, we can say that DAI is a function of distortion and not of dilatation (pressure).

The hypothesis is proposed that separate brain tissue parameters determine the intracranial pressure response and distortional strain response in typical blunt head impacts. Two separate models of TBI, investigating injury mechanisms based on skull bending and rigid skull rotation, have shown that:

- There is no correlation between the distortion and the dilatation (pressure).

We conclude that it is not sufficient to test/validate numerical (FE) models for pressure prior to using them to predict injury. In fact, as the intracranial pressure response is a hydrostatics type problem, controlled only by the density of the cerebrum (and the elastic moduli of the skull), better predictions of intracranial pressures can be obtained more readily with hand calculations than with FE models.

In the absence of strain data from cadaver impacts, numerical modellers can do little more than ensure that the shear material properties that they use are correct. However, in an authoritative review of the time dependent shear material properties of human brain, Donnelly (1998) shows that the short and long-term shear moduli (G_0 and G_∞) are in the region of 1 kPa. In a review of material parameters used in recent FE models, Bradshaw (2001) demonstrates that various authors have used values for the short and long-term moduli in the range 17 kPa to 528 kPa, which is inconsistent with the experimental data. The distortional strain, maximum principal strain and injury prediction capabilities of these earlier models are therefore in question.

CONCLUSIONS

- The high bulk modulus of neural tissue means that the positive pressures typically encountered in head impact do not produce large strains. Positive intracranial pressures of order 100 kPa are therefore probably of little consequence to TBI.
- The low shear modulus of neural tissue means that principal strains are controlled by shear deformations. Therefore, the shear strain response in FE models is of critical importance if such models are to be used to model TBI.
- A two-layer analytical model of TBI, incorporating a fluid model of the subarachnoid space with a small amount of elasticity to represent the trabeculae, shows that the shear properties of the brain may be varied over a wide range with very little effect on the pressure response.
- A coronal plane numerical model of blunt head impact has also shown that the shear properties of the brain may be varied over a considerable range with little effect on the pressure response.
- As there is no one-to-one relation between dilatation and distortion in head impacts lasting more than 2 ms, it is not sufficient to validate numerical (FE) models for pressure and then expect them to predict brain injury.

REFERENCES

[1] Bain, A. C., Billiar, K. L., Shreiber, D. I., *et al.* (1997). In vivo mechanical thresholds for traumatic axonal damage. In *Proceedings of the Impact Head Injury: Responses, Mechanisms, Tolerance, Treatment and Countermeasures*, AGARD, Neuilly-sur-Seine, France.

[2] Bain, A. C. and Meaney, D. F. (1999). Thresholds for mechanical injury to the in vivo white matter. In *Proceedings of the 43rd Stapp Car Crash Conference*, Society of Automotive Engineers, Warrendale, PA, USA.

[3] Bradshaw, D. R. S. (2001). Linear wave propagation in traumatic brain injury. PhD Thesis, University of Southampton.

[4] Bradshaw, D. R. S., Ivarsson, J., Morfey, C. L. and Viano, D. C. (2001). Simulation of acute subdural haematoma and diffuse axonal injury in coronal head impacts. *Journal of Biomechanics* 34, 85-94.

[5] Donnelly, B. R. (1998). Brain tissue material properties: a comparison of results. In *Proceedings of the 26th International Workshop on Biomechanics Research*.

[6] Gray, H. and Bannister, L. H. (1995). Gray's anatomy: The anatomical basis of medicine and surgery. Churchill Livingston, London, UK.

[7] Holbourn, A. H. S. (1943). Mechanics of head injuries. *Lancet* 2, 438-441.

[8] Holbourn, A. H. S. (1945). The mechanics of brain injuries. *Brit Med B* 3, 147-149.

[9] Altair Engineering Ltd (1998). HyperMesh.

[10] Ivarsson, J., Viano, D. C., Lovsund, P. and Aldman, B. (2000). Strain relief from the cerebral ventricles during head impact: experimental studies on natural protection of the brain. *Journal of Biomechanics* 33, 181-189.

[11] Livermore Software Technology Corporation (1999). LS-DYNA.

[12] Margulies, S. S., Thibault, L. E. and Gennarelli, T. A. (1990). Physical model simulations of brain injury in the primate. *Journal of Biomechanics* 23, 823-836.

[13] McElhaney, J. H., Roberts, V. L. and Hilyard, J. F. (1976). Properties of human tissues and components: nervous tissues. In *Handbook of Human Tolerance*. Automobile Research Institute, Tokyo, Japan.

[14] Meaney, D. F. and Thibault, L. E. (1990). Physical model studies of cortical brain deformation in response to high strain rate inertial loading. In *Proceedings of the International IRCOBI Conference on the Biomechanics of Impacts*.

[15] Nahum, A. M., Smith, R. and Ward, C. C. (1977). Intracranial pressure dynamics during head impact. In *Proceedings of the 21st Stapp Car Crash Conference*, Society of Automotive Engineers, Warrendale, PA, USA.

[16] Thomas, L. M., Roberts, V. L. and Gurdjian, E. S. (1967). Impact-induced pressure gradients along three orthogonal axes in the human skull. *Journal of Neurosurgery* 26, 316-349.

[17] Trosseille, X., Tarriere, C., Lavaste, F., *et al.* (1992). Development of a FEM of the human head according to a specific test protocol. In *Proceedings of the 36th Stapp Car Crash Conference*, Society of Automotive Engineers, Warrendale, PA, USA.

APPENDIX A – Analytical model derivation

Dispersion relations

The model has been set up so that waves of frequency ω are travelling along the boundary with trace wavespeed c_{t}. First, introduce the free-wave wavenumbers

$$\kappa = \omega / c_{\mathrm{d}}\,,\ \kappa' = \omega / c_{\mathrm{s}} \text{ and } \kappa'_{\mathrm{f}} = \omega / c_{\mathrm{sf}}\,. \qquad \text{(A1)}$$

The travelling-wave boundary condition imposes the same x_1 direction wavenumber on all waves, whereas the x_2 direction wavenumbers depend on the free-wave wavenumbers. Thus

$$k_1 = \omega / c_{\mathrm{t}}\,, \qquad k_2 = -\mathrm{j}\sqrt{k_1^2 - \kappa^2}\,, \quad \text{(A2a-b)}$$

with similar expressions for k'_2 and $k'_{2\mathrm{f}}$ using κ' and κ'_{f}. Note that $k_{2\mathrm{f}} = k_2$, since $c_{\mathrm{df}} = c_{\mathrm{d}}$.

The sign of the wavenumbers is chosen to ensure that waves are either propagating or evanescent in the positive x_2 direction.

Potentials and displacements

The displacement potentials above (superscript +) and below (superscript –) the interface between the solid half-space and the fluid layer are considered separately. The common factor $\mathbb{E} = \mathrm{e}^{\mathrm{j}(\omega t - k_1 x_1)}$ describes the (x_1, t) dependence for all the waves.

$$\phi^+ = \hat{w}_1 \mathrm{e}^{-\mathrm{j}k_2 x_2}\mathbb{E}\,, \qquad \text{(A3)}$$

$$\Psi^+ = \hat{w}_2 \mathrm{e}^{-\mathrm{j}k'_2 x_2}\mathbb{E}\,, \qquad \text{(A4)}$$

$$\phi^- = \left(\hat{w}_3 \mathrm{e}^{-\mathrm{j}k_2 x_2} + \hat{w}_4 \mathrm{e}^{\mathrm{j}k_2 x_2}\right)\mathbb{E}\,, \qquad \text{(A5)}$$

$$\Psi^- = \left(\hat{w}_5 \mathrm{e}^{-\mathrm{j}k'_{2\mathrm{f}} x_2} + \hat{w}_6 \mathrm{e}^{\mathrm{j}k'_{2\mathrm{f}} x_2}\right)\mathbb{E}\,. \qquad \text{(A6)}$$

The complex wave amplitudes $\hat{w}_i$ (i = 1 to 6) are the unknowns. Certain relationships between them are required by matching displacements and stresses at the interface between the two layers.

Solution

The displacement components are readily obtained from the Helmholtz decomposition (Equation 9). The dilatational and distortional components of the strain tensor are calculated from the expression

$$\varepsilon_{ij} = \frac{1}{2}\left(\frac{\partial u_i}{\partial x_j} + \frac{\partial u_j}{\partial x_i}\right), \qquad \text{(A7)}$$

and the components of the stress tensor σ_{ij} are related to the components of the strain tensor by

$$\sigma_{ij} = \lambda\delta_{ij}\varepsilon_{kk} + 2\mu\varepsilon_{ij}\,, \qquad \text{(A8)}$$

where δ_{ij} is the Kronecker delta, and λ and μ are the Lamé material constants.

The displacement and stress fields are continuous at $x_2 = 0$. There are therefore four matching conditions: Two displacement conditions and two stress conditions. The equations resulting from the matching conditions must be solved for $\hat{w}_i\,(i = 3,4,5,6)$ in terms of $\hat{w}_1$ and $\hat{w}_2$.

For a given frequency ω and wavenumber k_1 along the boundary, the total particle velocity vector on the boundary ($x_2 = -l$) can be expressed as $\boldsymbol{u}_{|-l} = \hat{\boldsymbol{v}}\mathbb{E}$. Thus, differentiation with respect to time of the displacement equations gives the components of the velocity vector $\hat{\boldsymbol{v}}$ at the boundary in terms of the complex wave amplitudes $\hat{w}_3$ to $\hat{w}_6$.

Substituting for $\hat{w}_3$ to $\hat{w}_6$ from the matching conditions and then solving for $\hat{w}_1$ and $\hat{w}_2$ leads to expressions for the wave potentials in the cerebrum that are simply unmanageable to present here. However, the full working for the steps above and the resulting potentials $\hat{w}_1$ and $\hat{w}_2$ can be found in Bradshaw (2001).

The expressions for the dilatation and maximum distortion are

$$\hat{z} = -\kappa^2\hat{w}_1, \qquad \text{(A9)}$$

where $\Delta = \hat{z}\mathbb{E}$, and (as a real, not phasor, variable)

$$\tilde{e} = \sqrt{\left[\mathrm{Re}\left\{\hat{d}\mathbb{E}\right\}^2 + \left[\mathrm{Re}\left\{\hat{e}\mathbb{E}\right\}^2\right]\right]}, \qquad \text{(A10)}$$

where $\tfrac{1}{2}\left(\varepsilon_{11} - \varepsilon_{22}\right) = \hat{d}\mathbb{E}$,

and $\varepsilon_{12} = \hat{e}\mathbb{E}$.

$$2\tilde{e}^2_{\mathrm{peak}} = \left|\hat{d}\right|^2 + |\hat{e}|^2 + \sqrt{\left|\hat{d}\right|^4 + |\hat{e}|^4 + 2\alpha\left|\hat{d}\right|^2|\hat{e}|^2} \qquad \text{(A11)}$$

where $\alpha = \cos\left(2\arg\hat{d} - 2\arg\hat{e}\right)$.

Dimensional analysis

Since the problem is linear for small $\hat{\boldsymbol{v}}$, each output variable $\left(\hat{z}, \hat{d}, \hat{e}\right)$ may be written in the form

$$\hat{z} = \hat{z}_1\hat{v}_1 + \hat{z}_2\hat{v}_2 = \hat{\boldsymbol{z}}\cdot\hat{\boldsymbol{v}}\,, \qquad \text{(A12)}$$

where the coefficients $\hat{z}_i$ are complex response functions that are independent of $\hat{\boldsymbol{v}}$ (as with $\hat{d}_i$ and $\hat{e}_i$). Then the list of physical variables that describe the solution may be summarised by

$$\begin{Bmatrix}\hat{z}_1\\ \hat{z}_2\\ \hat{d}_1\\ \hat{d}_2\\ \hat{e}_1\\ \hat{e}_1\end{Bmatrix} = \begin{Bmatrix}\hat{z}_1\\ \hat{z}_2\\ \hat{d}_1\\ \hat{d}_2\\ \hat{e}_1\\ \hat{e}_1\end{Bmatrix}\left\{\omega, k_1, l, \nu, c_{\mathrm{d}}, c_{\mathrm{s}0}, \eta_{\mathrm{s}}, c_{\mathrm{sf}0}\right\}. \qquad \text{(A13)}$$

As there are only two dimensions on the right hand side $[\mathrm{L},\mathrm{T}]$, the number of independent variables can be reduced from eight to six. This is achieved by using c_{d} and l as dummy (scaling) variables. The six input groups are obtained in the usual way and, after rearrangement for physical significance, we obtain

$$C = \frac{c_{\mathrm{s}0}}{c_{\mathrm{d}}} \quad \text{cerebral shear wavespeed ratio}$$

$$S = \frac{\omega l^2}{\nu} \quad \text{Stokes number}$$

$$Ma_{\mathrm{t}} = \frac{c_{\mathrm{t}}}{c_{\mathrm{d}}} \quad \text{trace Mach number}$$

$$Re = \frac{lc_{\mathrm{d}}}{\nu} \quad \text{Reynolds number}$$

$$\eta_{\mathrm{s}} = \eta_{\mathrm{s}} \quad \text{loss factor}$$

$$\gamma = \frac{c_{\mathrm{sf}0}}{c_{\mathrm{d}}} \quad \text{CSF shear wavespeed number}$$

The final dimensionless form is therefore

$$\begin{Bmatrix}\hat{Z}_1\\ \hat{Z}_2\\ \hat{D}_1\\ \hat{D}_2\\ \hat{E}_1\\ \hat{E}_2\end{Bmatrix} = \begin{Bmatrix}\hat{Z}_1\\ \hat{Z}_2\\ \hat{D}_1\\ \hat{D}_2\\ \hat{E}_1\\ \hat{E}_2\end{Bmatrix}\left\{C, S, Ma_{\mathrm{t}}, Re, \eta_{\mathrm{s}}, \gamma\right\}. \qquad \text{(A14)}$$